Solubility, Heat Capacity, and Density of Lithium Bromide + Lithium Iodide + Lithium Nitrate + Lithium Chloride Aqueous Solutions at Several Compositions and Temperatures

Daniel Salavera,[†] Xavier Esteve,[†] K. R. Patil,[†] Ana M. Mainar,[‡] and Alberto Coronas*[,†]

Center of Technological Innovation CREVER, Universitat Rovira i Virgili, Autovía de Salou s/n, 43006 Tarragona, Spain, and Group of Applied Thermodynamics and Surfaces (GATHERS), Aragon Institute for Engineering Research, Universidad de Zaragoza, 50009 Zaragoza, Spain

The lithium bromide + lithium iodide + lithium nitrate + lithium chloride (mole ratio 5:1:1:2) aqueous solution is a potential working fluid for air-cooled absorption chillers. Three important thermophysical properties were measured: solubility, heat capacity, and density. The solubilities were measured, in the temperature range (276.04 to 353.21) K, using visual polythermal and calorimetric methods. Heat capacities were measured in the range of temperatures from (312.63 to 372.08) K and a range of total salt mass fraction of (0.4953 to 0.6394). Liquid densities were measured at 1.0 MPa from (303.15 to 423.15) K and total salt mass fraction from (0.5150 to 0.6594). In addition, the Young's rule was checked for density predictions in the reported system at (305.15 and 323.15) K and 0.1 MPa. For this purpose, densities of the quaternary salt and lithium iodide aqueous solutions were measured at 0.1 MPa and several temperatures and concentrations. All the experimental data were correlated using empirical polynomial equations.

Introduction

The use of alternative refrigeration systems, such as the absorption-based one, is very suitable because it does not contribute to the depletion of the ozone layer. In recent years, a new concept related to the sustainable process led to the use of classical working pairs together with solar energy and waste heat in absorption technology;[1−4] this option does not increase the greenhouse effect. Water + lithium bromide systems have some drawbacks due to crystallization and corrosion at high temperature. To reduce these problems, some authors have suggested the use of several additives.[5−10] So, the presence of lithium chloride decreases the vapor pressure,[10] lithium iodide and lithium nitrate improve the solubility,[9] and lithium nitrate reduces corrosion in the system.[7] For these reasons, the aqueous solution of the quaternary salt system LiBr + LiI + LiCl + $LiNO_3$ presents favorable properties required for absorption chillers: less corrosion and lower crystallization temperature, about 35 K, than those for the water + lithium bromide solution. In 1999, Koo et al.[11] suggested the optimum mole ratio of salts in the molar proportion (5:1:1:2) LiBr + LiI + $LiNO_3$ + LiCl and determined some physicochemical properties. However, the essential and wide range data for several properties are needed to design and develop an absorption-based system.

To complete our previous works on the use of the LiBr + LiI + $LiNO_3$ + LiCl aqueous solution as a working fluid for air-cooled absorption chillers,[12,13] we report in this paper solubility, heat capacity, and density for the water + LiBr + LiI + $LiNO_3$ + LiCl (5:1:1:2) system. Solubility was measured at (276.04 to 353.21) K by using two methods well described in the literature,[14−16,1] the differential scanning calorimetry and visual polythermal methods. Heat capacities at (312.63 to 372.08) K and 0.1 MPa were measured by calorimetry for total salt mass fractions between 0.4953 and 0.6394. Densities of the quaternary salt system were obtained at 1.0 MPa for total salt mass fractions between 0.5150 and 0.6594 in the temperature range (303.15 to 423.15) K. All the experimental data were correlated with polynomial equations. Also, we have used Young's rule[17] to predict the density of the quaternary salt aqueous solution at atmospheric pressure from the density data of the single salt aqueous solutions. Since the density data for aqueous lithium iodide are scarce in the literature,[18] it was measured in the temperature range from (303.15 to 333.15) K for salt mass fractions from 0.14 to 0.27. The predicted density of the studied system was compared with the experimental one, measured in our laboratory, at atmospheric pressure.

Experimental Section

Materials. The salts used in this work were lithium bromide (Aldrich, 99+%), lithium iodide (Aldrich, 99%), lithium nitrate (Aldrich, 99+%), and lithium chloride (Aldrich, 99+%). Before use, all the salts except lithium iodide were heated under vacuum and dried at 353.15 K in an oven. The solutions were prepared using Millipore water ($\rho \leq 18.2$ MΩ·cm) previously degassed by several freezing−thawing cycles. As reference compounds, we used benzene (Panreac, 99.8%) and dry nitrogen for density measurements; potassium chloride (Scharlau, 99.5%) for solubility; and heptane (Fluka, >99.5%), ethanol (Panreac, >99.5%), and 1-octanol (Fluka, >99.5%) for heat capacities.

Equipment and Procedure. (a) Solubility. As pointed out, the salt solubilities were determined in two different ways: using a visual polythermal method and differential scanning calorimetry.

* To whom all correspondence should be addressed. E-mail: crever@crever.urv.es. Fax: +34-977-542272.
[†] Universitat Rovira i Virgili.
[‡] Universidad de Zaragoza.

10.1021/je034202x CCC: $27.50
Published on Web 03/04/2004

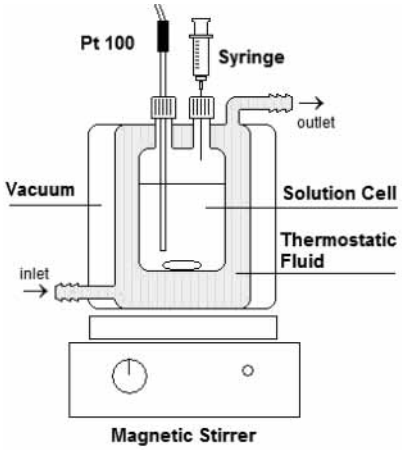

Figure 1. Scheme of the solution cell used in the visual polythermal technique.

The visual polythermal method (VP) is based on the observation of the temperature of desolution of the last crystal in a saturated solution. The experimental setup includes an equilibrium cell and a thermostat bath. In our case, the experimental device consists of a 40 mL cell with a double jacket made of Pyrex glass (Figure 1). The thermal fluid flows through the middle layer, and the external jacket, hermetically closed under vacuum to prevent fogging on the surface, acts as insulating material. The temperature in the cell was measured by means of a digital precision thermometer (Anton Paar MKT100) with a platinum thermoresistance PT 100. The accuracy of the temperature measurement is greater than ±0.01 K. The experimental technique has been described in the literature.[16,19] This process gives the equilibrium saturation temperature when the last crystal dissolves.

A heat flux Calvet-type calorimeter (Setaram C80) was used to tune the differential scanning calorimetry (DSC). The operation range for the calorimeter is from 5 K above the ambient temperature to 573 K, and the detection limit is 10 μW. For this use, the calorimeter was equipped with a reversal mixing mechanism and with specific cells (capacity: 4 mL) made in Hastelloy C.

The samples were prepared in the cell at room temperature by mass using a Mettler AE260 analytical balance with a precision of $\pm 10^{-4}$ g. The uncertainty of the salt mass fraction was estimated to be ±0.0001. Before the cell was placed in the calorimeter block, it was heated and stirred vigorously by hand to dissolve the salts. Once the cell is in the block, the reversal mixing mechanism is activated to ensure a higher homogeneity of the solution during the experiment. The solution is kept at constant temperature in the calorimeter for a long time (between 5 and 6 h) to stabilize the heat flow (±0.02 mW). Finally, the system is heated at 0.05 K·min^{-1} up to a temperature higher than the expected solubility.

In this method, the solubility was determined from the heat flow signal. When the last crystal disappears, the increase of temperature in the calorimeter generates a thermal imbalance, manifested as an abrupt change in the heat flow signal. Solubility is calculated by the software package taking into account the glass transition signal. For this purpose, several consecutive cycles were programmed with decreasing heating or cooling rates. The uncertainty of the experimental temperature is estimated to be within ±0.02 K. A more detailed description of the process is given by Salavera.[20]

(b) Heat Capacity. The measurement of the isobaric heat capacity was also made by calorimetry using two vessels made of stainless steel with a special design to avoid the presence of any vapor phase. The isobaric heat capacity was measured using the step method. The heating rate was 0.3 K·min^{-1}. Ethanol and *n*-heptane were the fuids used to calibrate the calorimeter, and to check the experimental procedure, the liquid heat capacity of 1-octanol was determinated, and the results were compared with the recommended heat capacity data of Zábranský et al.[21] in the same temperature range. The uncertainty of the experimental heat capacities is $\pm 8 \times 10^{-3}$ J·g^{-1}·K^{-1}. The procedure used also was described in a previous work.[22]

(c) Density. Densities of solutions at atmospheric pressure and at 1.0 MPa were measured using an Anton Paar vibrating tube densimeter (DMA60/512 P). The pressure was applied to the system by means of nitrogen gas and regulated with a pressure generator (HiP 50-6-15). The pressure was controlled with a pressure transducer SETRA C280E, with the accuracy ±0.11% . The vibrating tube temperature was adjusted with a Julabo F20 thermostat and read by means of a digital precision thermometer (Anton Paar MKT100) with a platinum thermoresistance PT 100. Millipore water and nitrogen gas were used as reference fluids for the calibration of the densimeter. To check the densimeter and the experimental procedure, the liquid densities of ethanol and *n*-octane at 1 MPa pressure were measured in the range (283.15 to 423.15) K and compared with the measurement of Cibulka and Hnedkovsk[23] and the *TRC Tables*.[24] The accuracy of the temperature measurement is ±0.015 K, and the uncertainty for the measured densities is $\pm 4 \times 10^{-1}$ kg·m^{-3}. The procedure followed was described in a previous work.[22]

Results and Discussion

Solubility. To validate the two methods described to determine the salt solubility, potassium chloride water solutions of total salt mass fractions (0.2700 to 0.3053) were selected as reference material.[25] The root-mean-square relative deviation (RMSD) between experimental and literature solubility values is 0.62% for the VP method and 1.65% for the DSC method. The RMSD is defined as

$$\mathrm{RMSD} = 100\left\{\frac{1}{N}\sum_i \left(\frac{X_e - X_{c/b}}{X_e}\right)_i^2\right\}^{1/2} \qquad (1)$$

where N, X_e, and $X_{c/b}$ are the number of data points and the experimental and calculated/bibliographic values, respectively.

To compare with the case of the quaternary salt system, the solubility of H_2O + LiBr in the concentration range of total salt mass fraction (0.5800 to 0.6627) was also measured. Table 1 shows the experimental results together with the literature data.[26] The RMSD values were lower than 1.3% for the VP method and 3.2% for the DSC method.

The solubilities obtained for H_2O + LiBr + LiI + $LiNO_3$ + LiCl using the two experimental techniques (VP and DSC) are gathered in Table 2. In this table, the values obtained from the equation proposed by Koo et al.[16] are also included. The maximum relative deviations between our experimental data and those calculated using the correlation of Koo et al.[16] are 2.3% and 3.1% for the VP and DSC methods, respectively.

Figure 2 shows the experimental data reported in this work for water + lithium bromide and the quaternary aqueous salt system.

Table 1. Saturation Temperatures of H_2O (1) + LiBr (2) Determined by Using the Visual Polythermal Method (VP) and Digital Scanning Calorimetry (DSC), in the Mass Fraction (w_2) of LiBr Ranges (0.5800 to 0.6647) and (0.6199 to 0.6725), Respectively, and the Comparison with Literature Data

experimental method	w_2	T/K	w_2	T/K
VP	0.5800	278.80	0.6351	313.01
		282.87[a]		311.68[a]
	0.5900	289.01	0.6400	313.71
		287.93[a]		314.73[a]
	0.5951	292.05	0.6453	318.05
		290.48[a]		318.23[a]
	0.6001	295.85	0.6495	321.04
		292.97[a]		321.19[a]
	0.6052	299.00	0.6428	314.55
		295.52[a]		316.55[a]
	0.6099	301.95	0.6532	325.91
		297.89[a]		323.94[a]
	0.6151	304.57	0.6559	330.41
		300.56[a]		326.04[a]
	0.6196	306.62	0.6593	335.26
		302.92[a]		328.81[a]
	0.6250	307.99	0.6628	341.28
		305.84[a]		331.81[a]
	0.6298	311.04	0.6647	343.16
		308.55[a]		333.51[a]
DSC	0.6199	306.15	0.6580	336.05
		303.08[a]		327.73[a]
	0.6248	307.57	0.6617	343.18
		305.73[a]		330.85[a]
	0.6510	326.07	0.6660	354.77
		322.29[a]		334.71[a]
	0.6556	331.07	0.6725	358.26
		325.80[a]		341.07[a]

[a] Reference 26.

Table 2. Saturation Temperatures of the LiBr + LiI + $LiNO_3$ + LiCl (Mole Ratio 5:1:1:2) + H_sO System Determined Using the Visual Polythermal Method (VP) and Digital Scanning Calorimetry (DSC) in the Mass Fraction (w_T) of Salt Ranges (0.6226 to 0.6961) and (0.6590 to 0.6995), Respectively, and the Comparison with Literature Data

experimental method	w_T	T/K	w_T	T/K
VP	0.6226	276.04	0.6654	315.85
		275.78[a]		306.12[a]
	0.6302	280.17	0.6700	321.83
		279.00[a]		311.21[a]
	0.6370	284.97	0.6772	329.15
		281.58[a]		319.18[a]
	0.6424	287.89	0.6799	332.69
		283.47[a]		322.01[a]
	0.6466	290.15	0.6848	337.56
		284.84[a]		327.18[a]
	0.6514	295.56	0.6906	344.04
		289.47[a]		333.03[a]
	0.6555	303.69	0.6961	348.15
		294.37[a]		338.45[a]
	0.6599	309.50		
		299.69[a]		
DSC	0.6590	305.77	0.6838	336.23
		298.66[a]		326.15[a]
	0.6656	317.16	0.6898	341.35
		306.41[a]		332.22[a]
	0.6699	323.96	0.6928	345.44
		311.22[a]		335.19[a]
	0.6767	327.83	0.6995	353.21
		318.64[a]		341.80[a]

[a] Reference 16.

Heat Capacity. The liquid heat capacities at 0.1 MPa constant pressure were measured in the temperature range from (313.15 to 373.15) K, at intervals of 10 K, for the total salt mass fractions (0.4953 to 0.6394). The experimental data, listed in Table 3, were correlated by the following polynomial equation, where w_T is the mass fraction of total salt:

$$C_p/\mathrm{kJ\cdot kg^{-1}\cdot K^{-1}} = \sum_{n=0}^{3}[A_n + B_n(T/\mathrm{K}) + C_n(T/\mathrm{K})^2](100w_T)^n \quad (2)$$

Table 4 summarizes the values of A_n, B_n, and C_n. The experimental and calculated data are plotted in Figure 3. The heat capacity increases with temperature and decreases with the total salt concentration. When our values are compared with those of Koo et al.,[16] the RMSD is 0.68%.

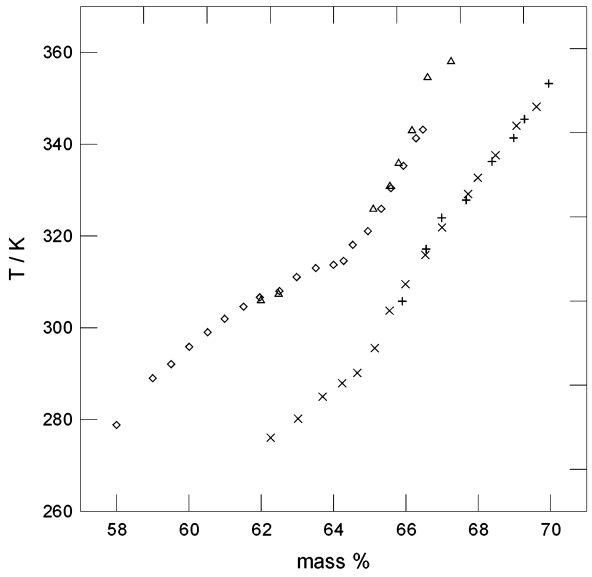

Figure 2. Solubilities of the lithium bromide aqueous salt systems. Experimental H_2O + LiBr: ◇, VP; △, DSC. Experimental LiBr + LiI + $LiNO_3$ + LiCl (mole ratio 5:1:1:2): ×, VP; +, DSC.

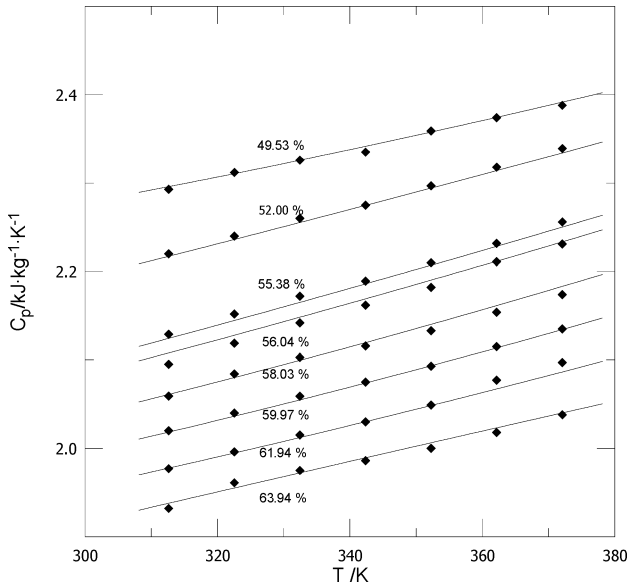

Figure 3. Heat capacity of LiBr + LiI + $LiNO_3$ + LiCl (mole ratio 5:1:1:2) + H_2O at 0.1 MPa, (49.53−63.94) mass %, and (312.64−372.08) K: ◆ experimental values; —, values calculated using eq 2.

Table 3. Experimental Heat Capacities of the LiBr + LiI + $LiNO_3$ + LiCl (Mole Ratio 5:1:1:2) + H_2O System at 0.1 MPa in the Mass Fraction of Salt (w_T) Ranges (0.4953 to 0.6394) and (312.64 to 372.08) K and the Comparison with Literature Data

	c_p/kJ·kg^{-1}·K^{-1}						
w_T	T = 312.63 K	T = 322.54 K	T = 332.45 K	T = 342.35 K	T = 352.26 K	T = 362.17 K	T = 372.08 K
0.4953	2.293	2.312	2.326	2.335	2.359	2.374	2.388
0.5200	2.220	2.240	2.260	2.275	2.297	2.318	2.339
	2.205[a]	2.214[a]					
0.5538	2.129	2.152	2.172	2.189	2.210	2.232	2.256
	2.127[a]	2.134[a]					
0.5604	2.095	2.119	2.142	2.162	2.182	2.211	2.231
	2.112[a]	2.118[a]					
0.5803	2.059	2.084	2.103	2.116	2.133	2.154	2.174
	2.066[a]	2.070[a]					
0.5997	2.020	2.040	2.059	2.075	2.093	2.115	2.135
	2.022[a]	2.024[a]					
0.6194	1.977	1.996	2.015	2.030	2.049	2.077	2.097
	1.979[a]	1.980[a]					
0.6394	1.932	1.961	1.975	1.986	2.000	2.018	2.038
	1.936[a]	1.939[a]					

[a] Reference 16.

Table 4. Fitting Coefficients and Standard Deviation of Eq 3 for the Heat Capacities of LiBr + LiI + $LiNO_3$ + LiCl (Mole Ratio 5:1:1:2) + H_2O at 0.1 MPa in the Mass Fraction of Salt (w_T) Ranges (0.4953 to 0.6394) and (312.64−372.08) K

n	A_n	B_n	RMSD
0	12.933	−0.024975	0.24
1	−0.38075	9.544×10^{-4}	
2	3.139×10^{-3}	-8.412×10^{-6}	

Density. The liquid densities at 1.0 MPa were measured in the range of temperatures from (303.15 to 423.15) K, at 20 K intervals, for total salt concentrations roughly of mass fraction from (0.50 to 0.65). The experimental data are listed in Table 5, and they were fitted using a polynomial equation dependent on the temperature and salt mass fraction by a least-squares method:

$$\rho/\mathrm{kg\cdot m^{-3}} = \sum_{n=0}^{3}[A_n + B_n(T/\mathrm{K}) + C_n(T/\mathrm{K})^2](100w_T)^n \quad (3)$$

where w_T is the mass fraction of total salt. The values of A_n, B_n, and C_n are shown in Table 6. The experimental and

Table 5. Experimental Densities of the LiBr + LiI + $LiNO_3$ + LiCl (Mole Ratio 5:1:1:2) + H_2O System at 0.1 MPa and 1.0 MPa in the Salt Mass Fraction (w_T) Ranges (0.5150 to 0.6595) and (303.15 to 423.15) K and the Comparison with Literature Data

	ρ/kg·m^{-3}						
w_T	T = 303.15 K	T = 323.15 K	T = 343.15 K	T = 363.15 K	T = 383.15 K	T = 403.15 K	T = 423.15 K
				P = 0.1 MPa			
0.5150	1517.7	1505.7	1493.2	1480.4	1466.9	1453.0	
	1510[a]	1499[a]					
0.5279	1535.7	1524.1	1511.8	1499.5	1486.4	1472.9	
	1530[a]	1518[a]					
0.5650	1595.5	1583.0	1570.7	1557.7	1546.3	1532.1	1518.1
	1587[a]	1575[a]					
0.5808	1624.1	1611.3	1598.1	1584.9	1571.6	1557.7	1543.4
	1613[a]	1601[a]					
0.5944	1648.8	1635.7	1622.1	1608.5	1592.5	1577.9	1563.7
	1637[a]	1624[a]					
0.6000	1658.8	1645.8	1632.1	1618.3	1602.5	1587.8	1573.4
	1647[a]	1633[a]					
0.6101	1678.8	1665.5	1651.6	1637.6	1621.5	1606.7	1592.2
	1665[a]	1652[a]					
0.6256	1708.3	1694.8	1705.9	1666.0	1649.7	1634.6	1619.9
	1695[a]	1681[a]					
0.6438	1744.4	1730.5	1715.5	1700.9	1681.8	1666.3	1651.3
	1733[a]	1718[a]					
0.6594	1773.9	1758.8	1743.2	1728.4	1710.1	1694.3	1677.3
				P = 1.0 MPa			
0.5150	1508.5	1497.4	1484.9	1472.7	1460.2	1446.3	1433.1
0.5280	1531.1	1521.4	1509.2	1495.7	1483.4	1469.5	1455.9
0.5498	1572.2	1561.2	1548.6	1536.3	1521.3	1508.4	1495.1
0.5650	1592.9	1580.4	1568.7	1555.1	1541.5	1526.8	1511.8
0.5807	1625.0	1611.7	1599.1	1585.7	1571.5	1556.7	1541.9
0.5944	1651.0	1637.9	1625.3	1612.1	1596.6	1582.1	1570.2
0.6000	1666.9	1654.2	1639.1	1624.6	1610.9	1597.4	1583.1
0.6100	1686.8	1671.4	1657.8	1643.7	1629.0	1613.7	1598.5
0.6263	1710.2	1695.3	1681.2	1666.5	1651.7	1636.4	1621.1
0.6437	1750.1	1734.5	1720.1	1705.0	1689.7	1673.7	1658.0
0.6594	1794.2	1775.9	1761.0	1745.4	1728.9	1712.3	1696.3

[a] Reference 11.

Table 6. Fitting Coefficients and Standard Deviations of Eq 4 for the Densities of LiBr + LiI + $LiNO_3$ + LiCl (Mole Ratio 5:1:1:2) + H_2O at 0.1 MPa and 1.0 MPa for the Mass Fraction of Salt Range (w_T) (0.5150 to 0.6595) and (303.15−423.15) K

$P = 1.0$ MPa				
n	A_n	B_n	C_n	RMSD
0	2008	−2.501		0.20
1	−27.41	0.07438		
2	0.3944	-5.99×10^{-4}	-1.98×10^{-7}	
$P = 0.1$ MPa				
n	A_n	B_n	C_n	RMSD
0	1810	−1.754		0.21
1	−21.51	0.0481		
2	0.3773	-5.11×10^{-4}		

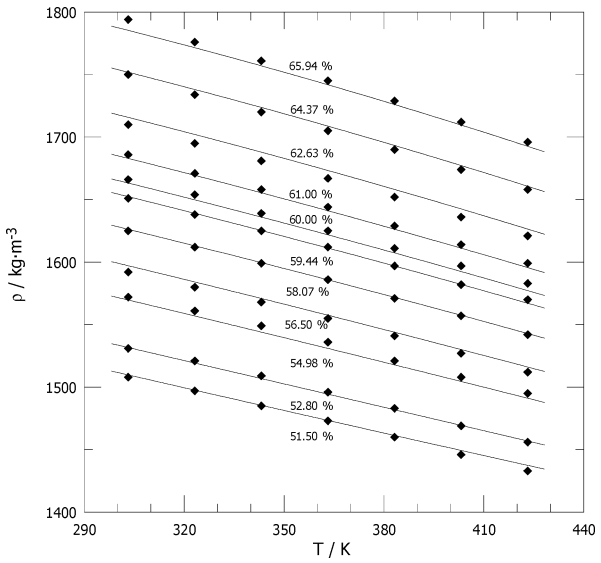

Figure 4. Densities of LiBr + LiI + $LiNO_3$ + LiCl (mole ratio 5:1:1:2) + H_2O at 1.0 MPa, (51.50−65.95) mass %, and (303.15−423.15) K: ◆, experimental values; —, values calculated using eq 3.

calculated data are plotted in Figure 4. The RMSD value between the experimental data of this work and the corresponding ones from the equation proposed by Koo et al.[11] is 0.64%. It can be observed that density increases with the salt concentration and decreases with temperature.

Finally, densities at 0.1 MPa for the quaternary salt solution and for the lithium iodide aqueous solution are reported (Tables 5 and 7). When our results are compared with the data available in the literature, a RMSDs of 0.08% and 0.66% are achieved, respectively, for the LiI + H_2O and LiBr + LiI + $LiNO_3$ + LiCl + H_2O systems at 0.1 MPa. The experimental results are also fitted using eq 3, and the corresponding coefficients appear in Tables 6 and 8. The main objective of this new experimental data set is to test Young's rule as a useful method for predicting density in practical applications.

In 1954, Young and Smith[17] suggested a connection between the apparent molar volume (V_ϕ) of a mixed electrolyte solution and the apparent molar volumes of its constituent binary subsystems ($V_{\varphi,i}$) through

$$V_\varphi/\mathrm{cm^3\cdot mol^{-1}} = \frac{\sum_i n_i V_{\varphi,i}}{\sum_i n_i} \tag{4}$$

and between the apparent molar volumes and the density through

$$V_{\varphi,i}/\mathrm{cm^3\cdot mol^{-1}} = \frac{1000(d_w - d_i)}{d_w d_i m_i} + \frac{M_i}{d_i} \tag{5}$$

$$V_\varphi/\mathrm{cm^3\cdot mol^{-1}} = \frac{1000(d_w - d)}{d d_w m_T} + \frac{M_T}{d} \tag{6}$$

where d_w is the density of water at 298.15 K, d_i is the density of the constituent binary solutions, d is the density of the mixed electrolyte solution, $m_T = \sum_i m_i$ is the total molality of the mixture, and $M_T = \sum_i n_i M_i / \sum_i n_i$ is the mean molar mass of the solutes present. The combination of eqs 4−6 yields Young's density rule

$$d/\mathrm{g\cdot cm^{-3}} = \frac{M_T + 1000/m_T}{\sum_i \left[x_i \frac{1000(d_w - d_i)}{d_w d_i m_i} + \frac{M_i}{d_i} \right] + \frac{1000}{m_T d_w}} \tag{7}$$

with $x_i = n_i/\sum_i n_i$. Recently, other authors have proposed several relations and empirical approaches for estimating the density in electrolyte solutions.[18,19]

Therefore, the density at 0.1 MPa of the quaternary system, LiBr + LiI + $LiNO_3$ + LiCl (molar ratio 5:1:1:2) + H_2O, has been predicted at 323.15 K and 343.15 K using the density equations proposed by Wimby and Berntsson[29] for the binary subsystems, H_2O + LiBr, H_2O + $LiNO_3$, and

Table 7. Experimental Densities of the H_2O (1) + LiI (2) Solution System at 0.1 MPa, Mass Fraction of LiI (w_2) (0.1496 to 0.2702), and (303.15−343.15) K and the Comparison with Literature Data

	ρ/kg·m^{-3}				
w_2	$T = 303.15$ K	$T = 313.15$ K	$T = 323.15$ K	$T = 333.15$ K	$T = 343.15$ K
0.1496	1118.2	1114.7	1109.3	1103.4	1095.5
	1118.0[a]				
0.1652	1132.5	1128.8	1121.9	1114.5	1108.2
	1132.5[a]				
0.1796	1145.3	1141.5	1135.7	1128.0	1120.2
	1146.1[a]				
0.2093	1174.6	1170.7	1164.7	1158.1	1149.3
	1175.2[a]				
0.2401	1205.1	1201.2	1195.0	1188.8	1181.7
	1206.9[a]				
0.2702	1238.6	1234.2	1228.2	1220.9	1213.9
	1239.4[a]				

[a] Reference 18.

Table 8. Fitting Coefficients and Standard Deviation of Eq 4 for the Densities of the H_2O + LiI Solution System at 0.1 MPa, Mass Fraction of Salt (w_T) (0.1496 to 0.2702), and (303.15−343.15) K

n	A_n	B_n	RMSD
0	−222.03	3.9052	0.09
1	211.92	−0.655981	
2	−9.6624	0.031046	
3	0.151048	-4.802×10^{-4}	

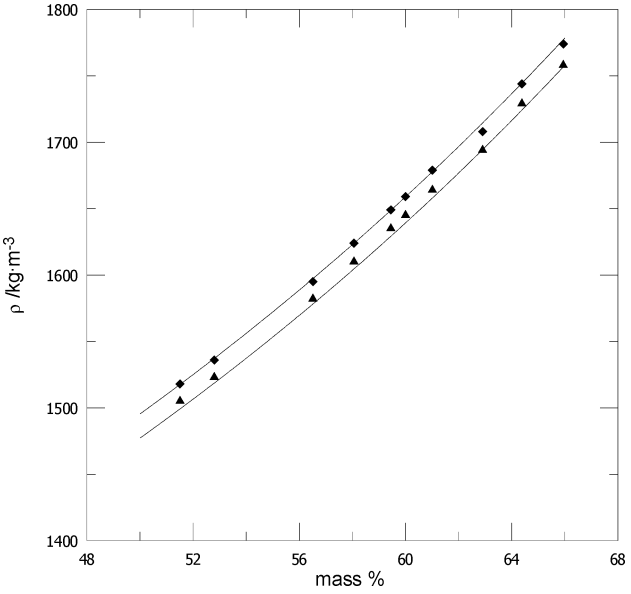

Figure 5. Experimental and predicted densities of LiBr + LiI + $LiNO_3$ + LiCl (mole ratio 5:1:1:2) + H_2O at 0.1 MPa and (51.50−65.95) mass %: ◆, experimental values at 303.15 K; ▲, experimental values at 323.15 K; −, values predicted using Young's rule.

H_2O + LiCl, with ours results for H_2O + LiI. Figure 5 shows the experimental and predicted densities for the system studied. The predicted values are lower than the experimental ones, but in all the cases the deviation is less than 0.85%.

Conclusions

Solubility, heat capacity, and density, three important thermophysical properties, have been determined for the system LiBr + LiI + $LiNO_3$ + LiCl (mole ratio 5:1:1:2) + H_2O at several working conditions.

In this paper, two experimental techniques have been used to determine the solubility of the salt system. The best results were obtained with the visual polythermal method, but differential scanning calorimetry is potentially more interesting due to its capacity to measure at higher temperatures (up to 573 K). In the future, further calorimetric studies will be done in order to achieve the most appropriate working conditions for these types of mixtures.

Heat capacities (at 0.1 MPa) and densities (at 0.1 and 1.0 MPa) have been measured up to 372.08 and 423.15 K, respectively.

Finally, the Young's rule appears as a practical method to predict the density of electrolyte multicomponent systems in the range of conditions established.

Literature Cited

(1) Haim, I.; Grossman, G.; Shavit, A. Simulation and Analysis of Open Cycle Absorption System for Solar Energy. *Sol. Energy* **1992**, *49*, 515−534.

(2) Merrick, R. H. Direct Evaporatively Cooled Three Ton Lithium Bromide-Water Absorption Chiller for Solar Application. *ASHRAE Trans.* **1982**, *88*, 797−809.

(3) Grossman, G.; Pérez-Blanco, H. Conceptual Dessing and Performance Analysis of Absorption Heat Pump for Waste Heat Utilization. *ASHRAE Trans.* **1982**, *88*, 451−466.

(4) Ma, W. B.; Deng, S. M. Theoretical Analysis of Low-Temperature Hot Source Driven Two-Stage LiBr/H_2O Absorption Refrigeration System. *Int. J. Refrig.* **1996**, *19*, 141−146.

(5) Hihara, E. Current Status of Thermophysical Property Research on New Working Fluids. *Refrigeration* **1993**, *68*, 693−698.

(6) Iyoki, S.; Iwasaki, S.; Kuriyama, Y.; Uemura, T. Integral Enthalpies of Mixing for Water + Lithium Bromide + Lithium Iodide and Water + Lithium Chloride + Lithium Nitrate at 298.15 K. *J. Chem. Eng. Data* **1993**, *38*, 299−301.

(7) Iyoki, S.; Yamanaka, R.; Uemura, T. Physical and Thermal Properties of the Water-Lithium Bromide-Lithium Nitrate System. *Int. J. Refrig.* **1993**, *16*, 191−200.

(8) Iyoki, S.; Iwasaki, S.; Kuriyama, Y.; Uemura, T. Densities, Viscosities, and Surface Tensions for the Two Ternary Systems Water + Lithium Bromide + Lithium Iodide + Lithium Chloride + Lithium Nitrate. *J. Chem. Eng. Data* **1993**, *38*, 302−305.

(9) Iyoki, S.; Iwasaki, S.; Kuriyama, Y.; Uemura, T. Solubilities of the Two Ternary Systems Water + Lithium Bromide + Lithium Iodide and Water + Lithium Chloride + Lithium Nitrate at Various Temperatures. *J. Chem. Eng. Data* **1993**, *38*, 396−398.

(10) Uemura, T. Working Medium-Absorbent Systems for Absorption Refrigeration Machine, Absorption Heat Pump and Heat Transformer. *Refrigeration* **1993**, *68*, 699−709.

(11) Koo, K. K.; Lee, H. R.; Jeong, S. Y.; Oh, Y. S.; Park, D. R.; Baek, Y. S. Densities, Viscosities, and Surface Tensions of the (Water + Lithium Bromide + Lithium Nitrate + Lithium Iodide + Lithium Chloride) System. *J. Chem. Eng. Data* **1999**, *44*, 1175−1177.

(12) Medrano, M.; Bourouis, M.; Coronas, A. Performance of an Absorption-Compression Heat Pump for Air Conditioning Using the System Water/LiBr+LiI+LiNO3+LiCl as Working Pair. *Proceedings of the ASME-ZSITS International Thermal Science Seminar*, Bled (Eslovenia), 2000; pp 515−520.

(13) Bourouis, M.; Medrano, M.; Coronas, A. Absorption in Falling Film on Vertical Tube Using Water/(LiBr+LiI+LiNO3+LiCl) in Air-Cooling Thermal Conditions. *Proceedings of the ZERO LEAKAGE-MINIMUM CHARGE, Efficient Systems for Refrigeration, Air Conditioning and Heat Pumps Conference*, Stockholm (Sweden), 2002; pp 243−251.

(14) Mohan, R.; Lorenz, H.; Myerson, A. S. Solubility Measurement Using Differential Scanning Calorimetry. *Ind. Eng. Chem. Res.* **2002**, *41*, 4854−4862.

(15) Young, P. H.; Schall, C. A. Cycloalkane Solubility Determination Through Differential Scanning Calorimetry. *Thermochim. Acta* **2001**, *367−368*, 387−392.

(16) Koo, K. K.; Lee, H. R.; Jeong, S. Y.; Oh, Y. S.; Park, D. R.; Baek, Y. S. Solubilities, Vapor Pressures and Heat Capacities of the Water + Lithium Bromide + Lithium Nitrate + Lithium Iodide + Lithium Chloride System. *Int. J. Thermophys.* **1999**, *20*, 589−600.

(17) Young, T. F.; Smith, M. B. Thermodynamic Properties of Mixtures of Electrolites In Aqueous Solutions. *J. Phys. Chem.* **1954**, *58*, 716−724.

(18) Patil, K. R.; Chaudhari, S. K.; Katti, S. S. Thermodynamic Properties of Aqueous Solutions of Lithium Iodide: Simplified Method for Preddicting the Enthalpies from the Vapor-Pressure Data. *Appl. Energy* **1991**, *39*, 189−199.

(19) Kim, J. S.; Lee, H. Solubilities, Vapor Pressures, Densities and Viscosities of the LiBr + LiI + $HO(CH_2)_3OH$ + H_2O System. *J. Chem. Eng. Data* **2001**, *46*, 79−83.

(20) Salavera, D. Determinación experimental de las densidades, solubilidades y viscosidades del sistema LiBr+$LiNO_3$+LiI+LiCl+H_2O. Tesis de Licenciatura, Universidad de Zaragoza. 2002.

(21) Zábranský, M.; Ruzicka, V.; Majer, Y. V. Heat Capacity of Liquids: Critical Review and Recomended Values. Vol. I and II. *J. Phys. Chem. Ref. Data* **1966**, Monograph 6.

(22) Esteve, X.; Conesa, A.; Coronas, A. Liquid Densities, Kinematic Viscosities, and Heat Capacities of Some Alkylene Glycol Dyalkil Ethers. *J. Chem. Eng. Data* **2003**, *48*, 392−397.

(23) Cibulka, I.; Hnedkovsk, L. Liquid Densities at Elevated Pressure of *n*-Alkanes from C5 to C16: A Critical Evaluation of Experimental Data. *J. Chem. Eng. Data* **1996**, *41*, 657−668.

(24) *TRC Thermodynamic Tables−Hydrocarbons*; Thermodynamic Research Center, Texax A&M University: Collage Station, TX, 1986.

(25) Potter, R. W.; Clynne, M. A. Solubility of Highly Soluble Salt in Aqueous Media−Part 1, NaCl, KCl, $CaCl_2$, Na_2SO_4, and K_2SO_4. Solubilities to 100 °C. *J. Res. U.S. Geol. Surv.* **1978**, *6*, 701−705.

(26) Boryta, D. A. Solubility of Lithium Bromide in Water Between −50° and +100° C. (45 to 70% Lithium Bromide). *J. Chem. Eng. Data* **1970**, *15*, 142−143.
(27) Miller, D. G. Connection Between Young's Rule for Apparent Molar Volumes and a Young's Rule for Density. *J. Solution Chem.* **1995**, *24*, 967−987.
(28) Hu, Y. F. An Empirical Approach for Estimating the Density of Multicomponent Aqueous Solutions Obeying the Linear Isopiestic Relation. *J. Solution Chem.* **2000**, *29*, 1229−1236.
(29) Wimby, J. M.; Berntsson, T. S. Viscosity and Density of Aqueous Solutions of LiBr, LiCl, $ZnBr_2$, $CaCl_2$ and $LiNO_3$. 1. Single Salt Solutions. *J. Chem. Eng. Data* **1994**, *39*, 68−72.

Received for review October 14, 2003. Accepted January 29, 2004. This work was financially supported by the Spanish National Research Program PROFIT (Energy Research Program Number 314- 2000).

JE034202X